Asian Journal of Chemistry; Vol. 34, No. 4 (2022), 931-936

ASIAN JOURNAL OF CHEMISTRY

https://doi.org/10.14233/ajchem.2022.23590

Crystallization Kinetics and Characterization of Solution Grown of Leucine Phthalic Acid Single Crystals

R. SENTHIL[1,2], G.V. VIJAYARAGHAVAN[1,*], M. ISMAIL FATHIMA[3], S. BEER MOHAMED[4] and A. AYESHAMARIAM[2]

[1]Department of Physics, B.S. Abdur Rahman Crescent Institute of Science and Technology, Chennai-600048, India
[2]Research Department of Physics, Khadir Mohideen College (affiliated to Bharathidasan University, Thiruchirappalli), Adirampattinam-614701, India
[3]PG and Research Department of Physics, Arul Anandar College, Karumathur, Madurai-625514, India
[4]Department of Material Science, Central University of Tamil Nadu, Thiruvarur-610001, India

*Corresponding author: E-mail: vijayaraghavan@crescent.education

Received: 19 October 2021; *Accepted*: 11 January 2022; *Published online*: 10 March 2022; AJC-20736

Single crystal of L-leucine phthalic acid was grown in slow evaporation technique at room temperature. The grown crystal is 7 mm × 2 mm × 1 mm in size. XRD, FT-IR, TG-DTA, UV, EDAX and SEM are all used to characterize a single crystal of L-leucine phthalic acid on dielectric characteristics, hardness and non-linear optical (NLO) properties. According to the findings, the effectiveness of L-LPA crystals is primarily determined by the surface quality of the crystals, which includes their capacity to resist high power intensities as well as their linear and non-linear optical characteristics.

Keywords: Slow evaporation method, NLO crystal, L-Leucine phthalic acid, Single crystal.

INTRODUCTION

In last three decades, non-linear optical (NLO) technology has gone a long way and NLO materials have gotten a lot of interest due to their unique properties. Optical systems that may be useful for high-speed data collection and messaging [1,2] are being developed in optoelectronics and optical data management. Recently, there has been a lot of buzz about new organic, inorganic and semi-organic NLO crystals [3].

The aggregation knowledge provided by the complexes, as well as the effect of other molecules on their aggregation molecular characteristics and interactions, has proven intriguing. Due to the dipolar nature, proteins have unique physical and chemical characteristics [4,5]. As a result, efforts to create amino acid mixed crystals suited for computer applications have been developed. The NLO characteristics can be seen in some organic or inorganic acid amino acid complexes [6,7]. L-leucine is an essential α-amino acid with a branched chain. The prospect of incorporating them in technical devices has piqued people's curiosity. L-Leucine has previously been studied in terms of growth and NLO and its SHG efficiency is double that of urea [8]. L-leucine nitrate [9], L-leucinium oxalate [10], *etc*. are few examples of L-leucine based NLO materials. Phthalate crystals are also frequently employed as diffracting crystals since they can easily split and might be used in a variety of devices [11-18]. As a result, this study details the synthesis and development of a single crystal of L-leucine phthalate, as well as characterizations such as XRD, FT-IR, TG-DTA, UV, EDAX and SEM. The results of experiments on dielectric characteristics, hardness and NLO are also discussed in depth.

EXPERIMENTAL

L-Leucine phthalic acid (L-LPA) single crystal was prepared using a 1:1 stoichiometric ratio of L-leucine ($C_6H_{13}NO_2$) and phthalic acid ($C_8H_6O_4$). The reactants were thoroughly dissolved in the necessary volume of water solution and vigorously agitated with a magnetic stirrer for 4 h. The solution was then filtered using Whatman filter paper and transferred to a petri plate, where crystallization was achieved by gently evaporating the solvent at room temperature. A high-grade seed, optically well-formed transparent crystals with dimensions of 7 mm × 2 mm × 1 mm were created from the saturated mother solution by continually draining the solvent over a 28 day period.

Characterization: After harvesting, the thermal stability, breakdown activity and water of hydration were investigated using the Perkin-Elmer TGA US automated recording instrument. In a N_2 environment, the sample was heated from 30 to 700 ºC at a rate of 10 ºC/min and the weight loss in percent was recorded. A PAN analytical X-ray diffractometer was used to report the powder XRD patterns of the samples. The powder XRD patterns of the materials were reported using Ni-filtered Cu*K*α radiation (λ = 1.5406 Å) and a scanning rate of 2 min^{-1}, 40 kV, 30 mA in a PAN analytical X-ray diffractometer. The FTIR spectra of the crystal in the wave number range 4000-400 cm^{-1} was obtained using the KBr pellet method in the Bruker Vector 22 spectrometer. A single L-leucine phthalate crystal's mechanical behaviour was examined. Vickers microhardness tests using a Leitz-Wetzler hardness tester fitted with a diamond pyramid indenter were used to examine the mechanical activity of the L-leucine phthalic acid single crystal. The AC electrical conductivity was measured in a pellet with a diameter of 10 mm and a thickness of 3 mm [19].

RESULTS AND DISCUSSION

Powder X-ray diffraction studies: Various planes of reflections of formed L-leucine phthalic acid (L-LPA) single crystal were discovered from powder X-ray diffraction pattern, as illustrated in Fig. 1. The XRD patterns for a single crystal of L-LPA show diffraction peaks of (001), (20$\bar{1}$), (002) and (310). The pattern vividly demonstrates the crystals' good crystalline nature. According to the findings, the prominent peak occurs at 27.132º, which is close to the (001) plane. The reference chemical crystallized in a monoclinic system with the non-centro symmetric space group. Sharp XRD pattern peaks demonstrated that the generated crystals had outstanding crystallinity, based on the placement of the diffraction peaks and the conclusion that they are crystalline in nature with a monoclinic system.

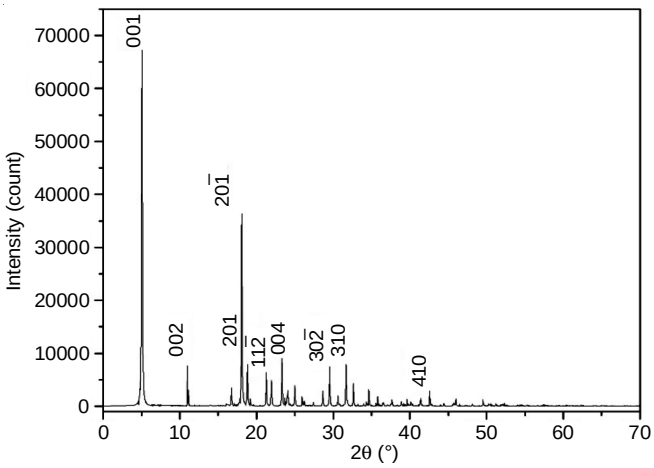

Fig. 1. XRD analysis of leucine crystals with phthalic acid

Using Scherrer equation's, the average crystallite size of a single crystal of L-LPA was calculated by using eqn. 1 [20]:

$$D = \frac{k\lambda}{\beta\cos\theta} \quad (1)$$

where k = 0.9 is a constant numerical form factor, D is the crystallite size, λ is the incident radiation wavelength, β is the FWHM in radians and θ is the Bragg angle in radians dislocation density (δ) was derived from crystallite size using eqn. 2 [20]:

$$\delta = \frac{1}{D^2} \quad (2)$$

Also strain (ε) of L-LPA single crystal was calculated using eqn. 3 [21]:

$$\varepsilon = \frac{\beta\cos\theta}{4} \quad (3)$$

The lattice constants a and c are the calculated values for monoclinic system structures:

$$\frac{1}{d^2} = \frac{h^2}{a^2\sin^2\gamma} + \frac{k^2}{b^2\sin^2\gamma} - \frac{2hk\cos\gamma}{ab\sin^2\gamma} + \frac{l^2}{c^2} \quad (4)$$

$$a \neq b \neq c,\ \alpha = \gamma = 90°,\ \beta \neq 90°$$

According to our current estimates, (001) planes have the largest X-ray irradiation area, which results in the highest peak intensity, which is similar to the peak indexed (20$\bar{1}$). As a result (Table-1), the most intense reflections are Miller-indexed (001) and (20$\bar{1}$), indicating that these are the crystal's preferred crystal planes. The absence of peaks for other forms of L-LPA in the XRD pattern confirms the crystallinity and purity of the generated crystals [20]. By indexing the various peaks in the diffractogram, the ideal values of interplanar spacing 'd' were obtained and compared to the conventional values [4]. The crystalline structure of a single crystal of L-leucine phthalic acid is shown in Fig. 2.

SEM studies: The nature and surface morphology of the L-LPA single crystal were investigated using SEM. Fig. 3 shows the surface shape and particle size of a formed crystal. The figure clearly shows that microcrystal particles are distributed uniformly over the surface of the crystal, which is practically smooth and free of fissures. This could be owing to the influence of optimal development conditions [22].

EDAX studies: EDAX analysis can be used to determine the qualitative and quantitative composition of elements and crystalline components of the grown crystal present in a sample. The resulting EDAX spectrum (Fig. 4) and Table-2 show the experimental weight percentages of elements (O, C, S and Si), confirmed the growth of the title compound [22,23].

TEM studies: Fig. 5a-b depicts the fluctuations in crystal count in saturated solutions of various ages. As can be seen,

TABLE-1
STRUTURAL PARAMETERS OF L-LPA SINGLE CRYSTAL

Sample	2θ (°)	hkl	d d (Å)	Crystallite size (nm)	Dislocation density ($\delta \times 10^{14}$ lines m^{-2})	Strain ($\varepsilon \times 10^{-5}$ lines^{-2} m^{-4})	Lattice constant (Å)		
							a	b	c
L-LPA single crystal	7.192	(001)	1.23	57	3.08	5.87	5.018	16.651	22.673

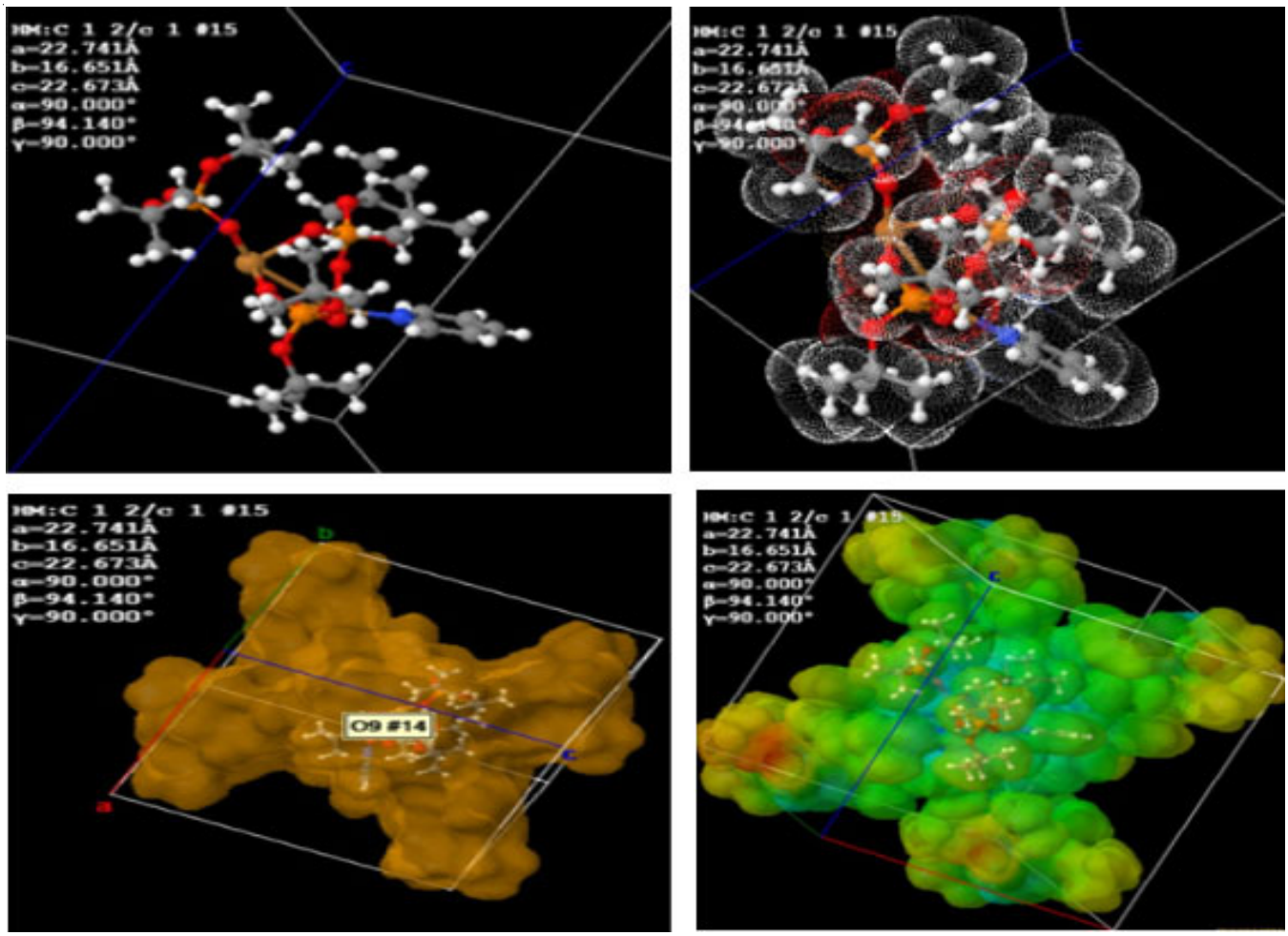

Fig. 2. Crystal structure of L-leucine phthalic acid (L-LPA) single crystal

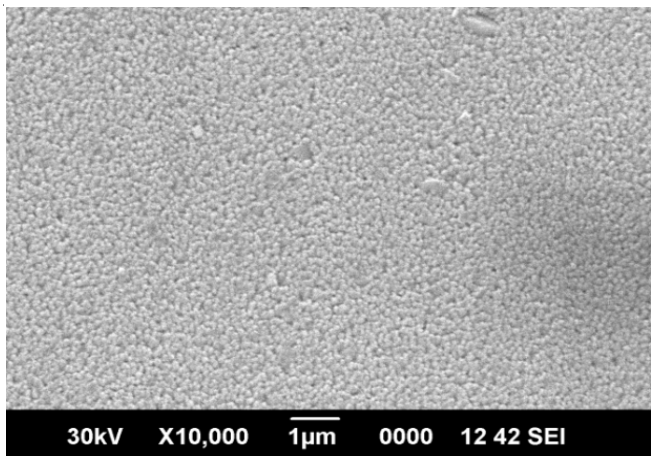

Fig. 3. SEM micrograph grown L-LPA single crystal

TABLE-2
EDAX ANALYSIS OF LEUCINE PHTHALIC ACID CRYSTALS

Element	keV	Mass (%)	At (%)
OK	0.525	14.39	44.91
C K	1.739	14.39	25.58
O L	3.285	57.66	25.08
S L	3.442	5.89	2.48
Si M	2.121	7.67	1.95
		100	100

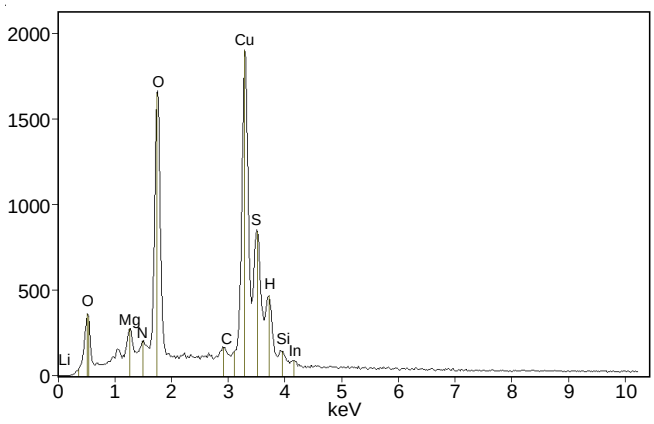

Fig. 4. EDAX analysis of leucine phthalic acid crystals

the nucleation rate falls as the solution ages and the pH rises. The reactant was carried through the solution in order to form crystals, resulting in regulated growth with fewer nucleation sites. The clarity of the crystal was only maintained in this study by using a slow evaporation procedure and keeping the pH of the solution at 4.5. Only the crystals extracted from the crystallizer with a solution pH of 4.5 and a 3 week solution aging period were further characterized [24]. Fig. 5b shows the SAED pattern of a single crystal of L-leucine phthalic acid.

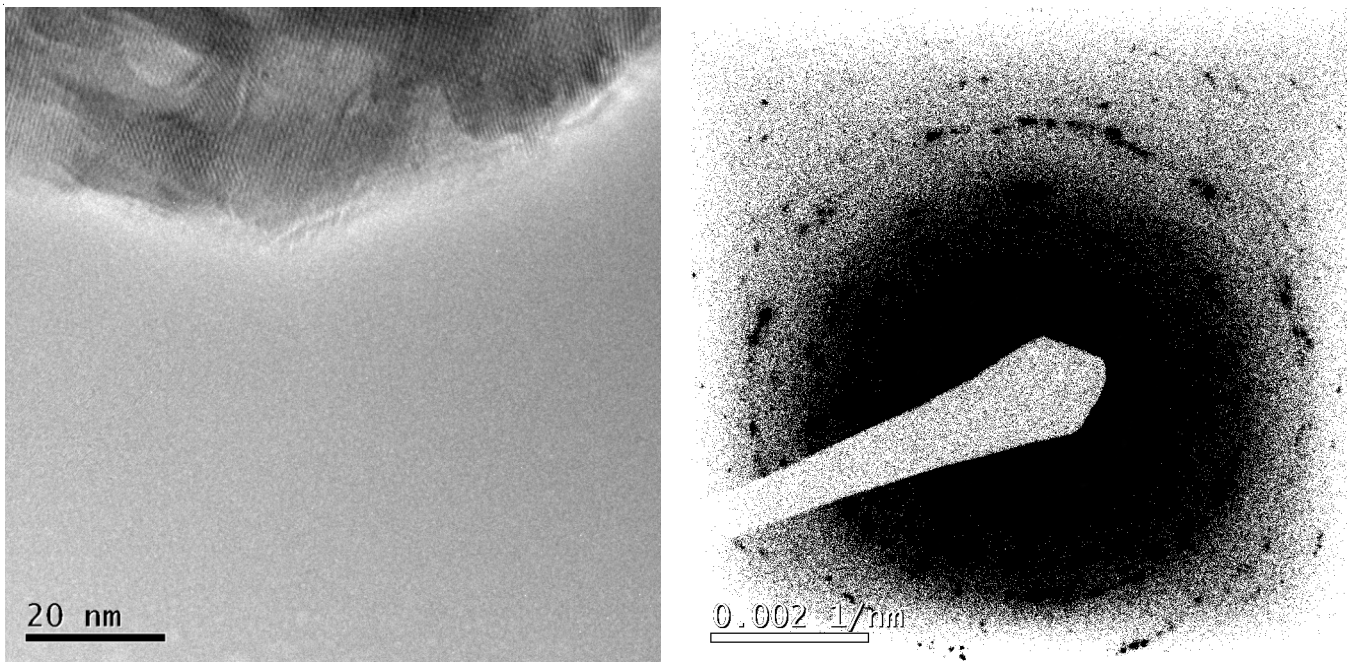

Fig. 5. (a) TEM (b) SAED pattern analysis of L-LPA

Vickers's hardness study: Hardness is associated to bond strength and crystal structure and material flexibility [25,26]. The crystals' Vickers hardness number (H_v) was obtained using the formula:

$$H_v = 1.8544 \frac{P}{d^2} \quad (kg/mm^2)$$

where d is the diagonal length of the depression and P is the weight applied in grams. The H_v variation for various loads demonstrates that the amount of hardness increases as the load increases up to 100 g. After 100 g, the crystal began to crack. Mayer's relation was used to derive the work hardening coefficient or Mayer's index (n), which connects the applied load to the indentation diagonal length.

$$P = Kd^n \text{ or } \log P = \log K + n \log d$$

where K stands for the material constant. The hardness number decreases as the load increases if n is less than 2 and it increases if n is more than 2. By plotting the curve of log p *vs*. log d as shown in Fig. 6, the job hardening coefficient 'n' was estimated to be 1.2 and found to be more than 1.6, suggesting that the crystal belongs to the soft material group [27].

The following equations are used to compute the young's modulus (E) and yield strength (Y). Table-3 shows the results of $E = 819635 \times H_v$ and $Y = H_v/3$. With increasing load, the crystals' young modulus and yield strength increase.

FTIR studies: The FTIR spectra of L-leucine phthalic acid at room temperature are shown in Fig. 7. We studied the molecular structure of L-leucine and phthalic acid as described in the literature [28,29] to evaluate the IR spectra. The main amine stretching bond is weak at 3442 cm^{-1} and 3243 cm^{-1} and there are stretching vibrations ascribed to the OH and NH groups. The methyl, amino and carboxyl functional groups were attributed to the peaks at 2935, 1503 and 1586 cm^{-1}, which are the typical IR peaks of L-leucine, respectively. The

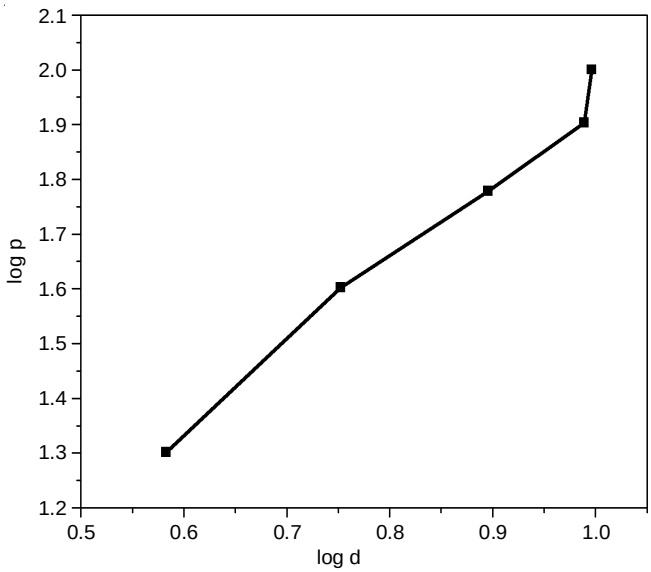

Fig. 6. Variation of diagonal length (log d) with load (log p)

TABLE-3
VICKER'S HARDNESS ANALYSES OF L-LUECINE PHTHALIC ACID (L-LPA) SINGLE CRYSTALS

Load P (g)	H_v (kg/mm^2)	$E = 81.9635 * H_v$	$y = H_v/3$
20	0.0467	3.8276	0.0155
40	0.069	5.6554	0.023
60	0.096	7.8684	0.032
80	0.119	9.7536	0.0396
100	0.121	9.9175	0.0403

asymmetric stretching vibration of the carboxyl ion COO^- is connected to the distinctive absorption band at 1586 cm^{-1}, whereas the comparatively faint absorption band at 2133 cm^{-1} corresponds to the NH frequencies of the NH_3^+ ion, indicating the dipolar nature. The ν(COO) stretching frequency of the

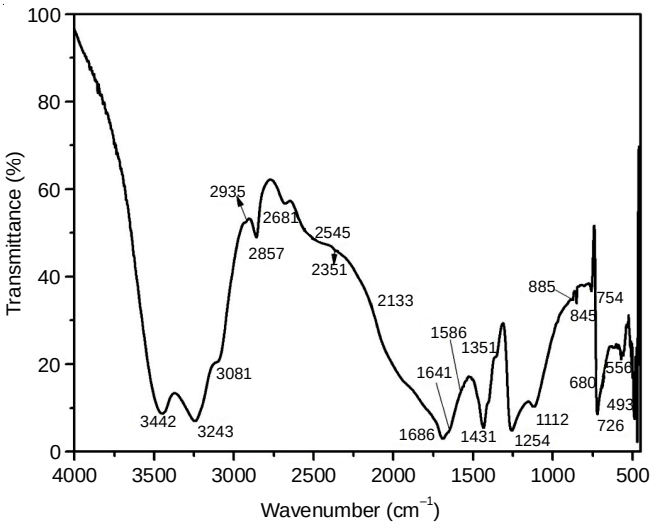

Fig. 7. FTIR anlysis of L-leucine phthalic acid crystals

carboxyl group of phthalic acid is presumably responsible for the absorption peaks at 1432 and 1586 cm^{-1}. The C-H stretching (superimposed on O-H stretching) in phthalic acid caused the absorption peak at 2857 and 2681 cm^{-1}. The strong absorption peak at 754 cm^{-1} shows orthodisubstitution in phthalic acid, whereas the other vibrational frequencies at 3007 and 1686 cm^{-1} are ascribed to the aromatic ring ν(C-H) and (C=C), respectively. In L-LPA, the disappearance of the phthalic acid absorption bands owing to O-H of the second carboxyl group in the range 2653-2527 cm^{-1} shows deprotonation of the ligand's one acidic group and the emergence of new bands at 680, 556 and 493 cm^{-1} in the spectra of complexes attributable to ν(N-O) as seen in the spectra of L-LPA indicates that the oxygen atoms have coordinated with the nitrogen ion and that the product has been produced. Both of these functional groups and bond vibrations confirmed the creation of L-LPA molecule.

Thermal studies: Thermogravimetric analysis (TGA) and differential thermogram analysis (DTA) give information on phase transitions and crystal breakdown phases. The TGA is carried out in a nitrogen atmosphere using a Perkin-Elmer thermal analyzer STA 409 PC with a heating rate of 2 ºC/min up to a temperature of 1000 ºC. The TGA and DTA spectra of L-LPA grown crystal are shown in Fig. 8. Crystals denied solvent molecules during crystallization because there was no weight loss below 245 ºC. This showed that the material was thermally stable enough for use in lasers because there was no breakdown up to melting point. The melting point of the crystal was discovered to be 245 ºC, where there was a rapid weight decrease with no intermediary stages. Weight loss happened in two stages, according to the TG curve. The breakdown of both compounds generated the first weight loss, which was 94.18%, while the evaporation of the organic component caused the second weight loss, which was 36.75%. The DTA curves revealed five endothermic peaks at 201.35, 329.42, 377.32, 495.86 and 553.78 ºC, all of which were linked with the TG, confirming the crystal's thermal stability [30].

Current-voltage and dielectric studies: The current-voltage characteristics of a single L-LPA crystal were investigated using an HP-Agilent 6268B Power Supply, a Keithley

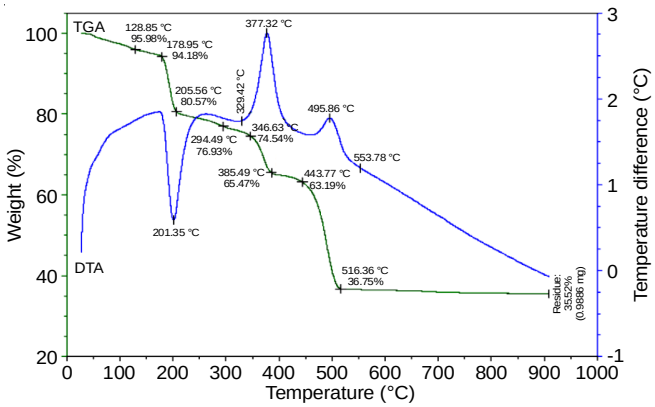

Fig. 8. TG/DTA analysis of L-LPA single crystal

6517A electrical meter and a HEWLETT 34401A electrical meter. The total transport current density for the developed L-LPA single crystal was described using four-terminal measurements as shown in Fig. 9. The highest current density at a voltage of 0.9 V is 0.6 Å [21,31].

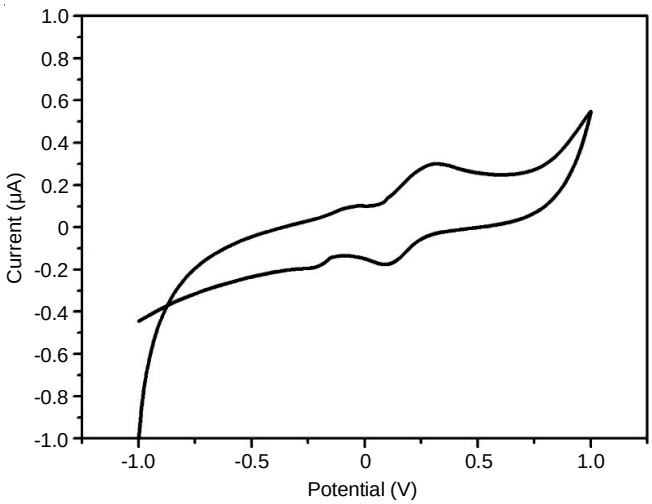

Fig. 9. C-V studies of L-LPA single crystal

The AC conductivity was also determined as a function of applied frequency. The observed difference is depicted in Fig. 10. It can be seen that as the frequency increases, so does the conductivity. At higher frequencies, interfacial polarization decreases, resulting in this feature. Because dielectric loss is less at higher frequencies, the formed crystal has a good optical efficiency and few flaws. In the use of NLO materials, this is a crucial parameter.

Second harmonic generation: The conversion efficiency for the second harmonic generation (SHG) was calculated utilizing the Kurtz-Perry technique since this grown L-LPA crystal contains a non-centrosymmetric space group. Before being exposed to a 1064 nm YAG laser beam, the L-LPA crystals were reduced to an uniform particle size. A powder of potassium dihydrogen orthophosphate (KDP) with the same particle size served as the control. A laser pulse of 8.8 mg was sent through powdered L-LPA sample, resulting in a 7.4 mJ second harmonic signal. According to this measurement, the SHG efficiency is 84% when compared to the KDP crystal.

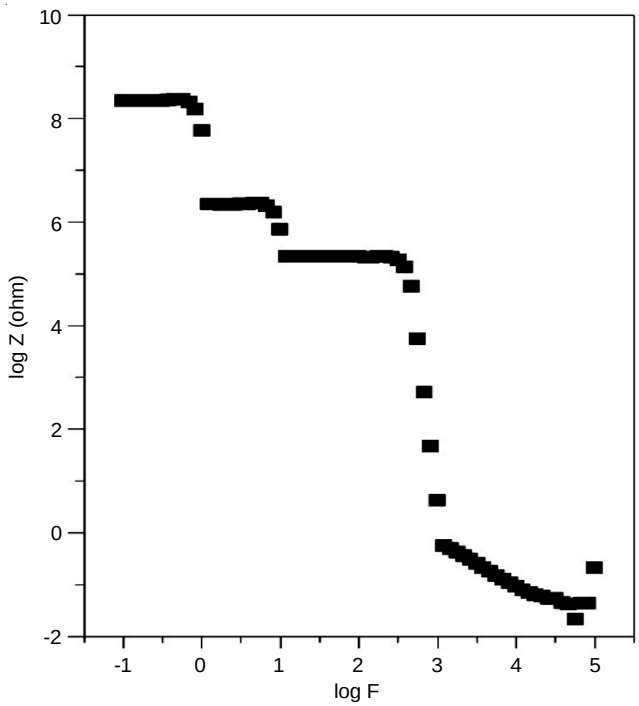

Fig. 10. Frequency dependence conductivity of (L-LPA) crystal

Conclusion

L-Leucine phthalic acid (L-LPA) single crystals were grown from an aqueous solution using a progressive evaporation method. Single crystal X-ray diffraction research was used to confirm the crystal system and lattice characteristics. The presence of functional groups in the title chemical was discovered by FT-IR analysis. According to studies, the grown crystal is thermally stable up to 345 ºC. The EDAX analysis confirmed the compound's structure and a surface inspection indicated that the produced crystals had a smooth surface. The dielectric constant dropped as frequency rose, according to dielectric studies. In a current-voltage study, the optical performance and non-linear applicability of generated L-LPA single crystals were demonstrated.

CONFLICT OF INTEREST

The authors declare that there is no conflict of interests regarding the publication of this article.

REFERENCES

1. D.F. Eaton, *Science*, **253**, 281 (1991); https://doi.org/10.1126/science.253.5017.281
2. S. Addanki, I.S. Amiri and P.Yupapin, *Results Phys.*, **10**, 743 (2018); https://doi.org/10.1016/j.rinp.2018.07.028
3. A.F. Garito, K.D. Singer and C.C. Teng, *ACS Symp. Ser.*, **233**, 1 (1983); https://doi.org/10.1021/bk-1983-0233.ch001
4. S.B. Monaco, L.E. Davis, S.P. Velsko, F.T. Wang, D. Eimerl and A. Zalkin, *J. Cryst. Growth*, **85**, 252 (1987); https://doi.org/10.1016/0022-0248(87)90231-4
5. G. Ravi, K. Srinivasan, S. Anbukumar and P. Ramasamy, *J. Cryst. Growth*, **137**, 598 (1994); https://doi.org/10.1016/0022-0248(94)91004-9
6. H. Bhat, *Bull. Mater. Sci.*, **17**, 1233 (1994); https://doi.org/10.1007/BF02747223
7. K.S. Thanthiriwatte and K.M. Nalin de Silva, *J. Mol. Struct.*, **617**, 169 (2002); https://doi.org/10.1016/S0166-1280(02)00419-0)
8. S. Adhikari and T. Kar, *Mater. Chem. Phys.*, **133**, 1055 (2012); https://doi.org/10.1016/j.matchemphys.2012.02.015
9. S. Adhikari and T. Kar, *J. Cryst. Growth*, **356**, 4 (2012); https://doi.org/10.1016/j.jcrysgro.2012.07.008
10. M.R. Jagadeesh, H.M.S. Kumar and R.A. Kumari, *Mater. Sci. Pol.*, **33**, 529 (2015); https://doi.org/10.1515/msp-2015-0063
11. G. Vasudevan, P. Anbu Srinivasan, G. Madhurambal and S.C. Mojumdar, *J. Therm. Anal. Calorim.*, **96**, 99 (2009); https://doi.org/10.1007/s10973-008-9880-7
12. K. Sathishkumar, J. Chandrasekaran, Y. Matsushita, A. Sato, C.I. Sathish, K. Yamaura and B. Babu, *Optik*, **126**, 981 (2015); https://doi.org/10.1016/j.ijleo.2015.02.079.
13. S. Suresh, *J. Electron. Mater.*, **45**, 5904 (2016); https://doi.org/10.1007/s11664-016-4798-5
14. A. Hemalatha, S. Arulmani, K. Deepa, D.S. Kumar, J. Madavan and S. Senthil, *Mater. Today Proc.*, **8**, 142 (2019); https://doi.org/10.1016/j.matpr.2019.02.092
15. J.E.M. Theras, D. Kalaivani, D. Jayaraman and V. Joseph, *J. Cryst. Growth*, **427**, 29 (2015); https://doi.org/10.1016/j.jcrysgro.2015.06.009
16. A. Senthil, P. Ramasamy and S. Verma, *J. Cryst. Growth*, **318**, 757 (2011); https://doi.org/10.1016/j.jcrysgro.2010.11.115
17. S. Trabattoni, L. Raimondo, A. Sassella and M. Moret, *J. Chem. Phys.*, **146**, 124701 (2017); https://doi.org/10.1063/1.4978236
18. A. Kassim, S. Nagalingam, H.S. Min and K. Noraini, *Arab. J. Chem.*, **3**, 243 (2010); https://doi.org/10.1016/j.arabjc.2010.05.002
19. N. Goel and B. Kumar, *J. Cryst. Growth*, **361**, 44 (2012); https://doi.org/10.1016/j.jcrysgro.2012.08.044
20. K. Sugandhi, S. Verma, M. Jose, V. Joseph and S.J. Das, *Optics Laser Technol.*, **54**, 347 (2013); https://doi.org/10.1016/j.optlastec.2013.05.028
21. A. Mishra, S.N. Choudhary, K. Prasad and R.N.P. Choudhary, *Phys. B*, **406**, 3279 (2011); https://doi.org/10.1016/j.physb.2011.05.040
22. R. Vivekanandhan, K. Raju, S. Sahaya Jude Dhas and V. Chithambaram, *Int. J. Appl. Eng. Res.*, **13**, 13454 (2010).
23. S. Gao, W. Chen, G. Wang and J. Chen, *J. Cryst. Growth*, **297**, 361 (2006); https://doi.org/10.1016/j.jcrysgro.2006.09.047
24. H.Q. Sun, D.R. Yuan, X.Q. Wang, X.F. Cheng, C.R. Gong, M. Zhou, H.Y. Xu, X.C. Wei, C.N. Luan, D.Y. Pan, Z.F. Li and X.Z. Shi, *Cryst. Res. Technol.*, **40**, 882 (2005); https://doi.org/10.1002/crat.200410450
25. J. Ramajothi, S. Dhanuskodi and K. Nagarajan, *Cryst. Res. Technol.*, **39**, 414 (2004); https://doi.org/10.1002/crat.200310204
26. S. Gao, W. Chen, G. Wang and J. Chen, *J. Cryst. Growth*, **297**, 361 (2006); https://doi.org/10.1016/j.jcrysgro.2006.09.047
27. L.-C. Zhang and H. Tanaka, *JSME Int. J. Series A*, **42**, 546 (1999); https://doi.org/10.1299/jsmea.42.546
28. X. Jiang, J. Zhao and X. Jiang, *Comput. Mater. Sci.*, **50**, 2287 (2011); https://doi.org/10.1016/j.commatsci.2011.01.043
29. M. Venkatesh, K.S. Rao, T.S. Abhilash, S.P. Tewari and A.K. Chaudhary, *Opt. Mater.*, **36**, 596 (2014); https://doi.org/10.1016/j.optmat.2013.10.021
30. A.J. Varjula, C. Vesta, C. Justin Raj, S. Dinakaran, A. Ramanand and S. Jerome Das, *Crystal Mater. Lett.*, **61**, 5053 (2007); https://doi.org/10.1016/j.matlet.2007.04.012
31. M.K. Mishra, *Chem. Sci. Trans.*, **5**, 770 (2016); https://doi.org/10.7598/cst2016.1260